

AD-A086 949

OAKLAND UNIV ROCHESTER MI SCHOOL OF ENGINEERING

F/G 20/11

EXPERIMENTAL ANALYSIS OF DISPLACEMENTS AND SHEARS AT THE SURFAC--ETC(U)

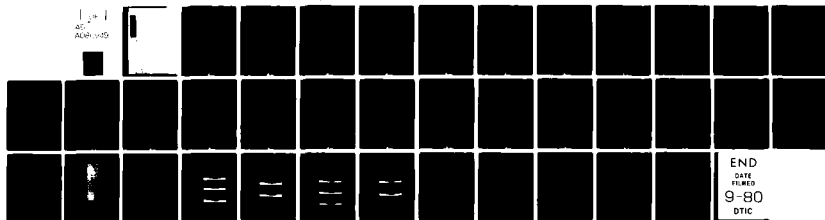
JUL 80 C BREMOND; A J DURELLI

N00014-76-C-0487

NL

UNCLASSIFIED 54

1-1
AD-A086 949



END
DATE
FILMED
9-80
DTIC

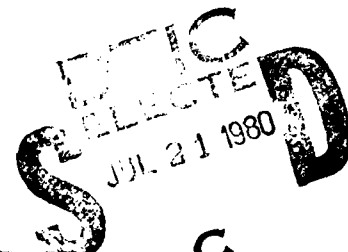
EXPERIMENTAL ANALYSIS OF DISPLACEMENTS AND SHEARS
AT THE SURFACE OF CONTACT BETWEEN TWO LOADED BODIES

by

(10) C. Brémond and A. J. Durelli

Sponsored by

Office of Naval Research
Department of the Navy
Washington, D.C. 20025



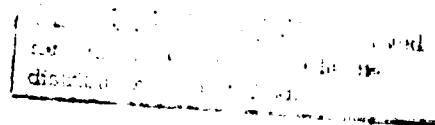
(15) N00014-76-C-0487
Contract No. N0014-76-C-0487
O.U. Project No. 31313-24

Report No. 54

(11) July 1980

(14) 12/38

School of Engineering
Oakland University
Rochester, Michigan 48063



405252

LB

EXPERIMENTAL ANALYSIS OF DISPLACEMENTS AND SHEARS
AT THE SURFACE OF CONTACT BETWEEN TWO LOADED BODIES

by C. Brémond and A.J. Durelli

TABLE OF CONTENTS

	Page
ABSTRACT	1
INTRODUCTION	1
CONSIDERATIONS ON THE OPTICAL METHODS.	2
ADVANTAGES OF THE GRID METHOD.	3
DESCRIPTION OF THE MODEL	4
TESTS.	5
ANALYSIS	6
RESULTS.	7
PRECISION OF THE RESULTS	9
LIMITATION OF THE METHOD	9
CONCLUSION	10
ACKNOWLEDGMENTS.	11
REFERENCES	12

Accession For	
NTIS GRA&I	<input checked="checked" type="checkbox"/>
DDC TAB	<input type="checkbox"/>
Unannounced	<input type="checkbox"/>
Justification	
By _____	
Distribution/_____	
Number of Copies _____	
Dist. _____	Available/or Special _____

A

Previous Technical Reports to the Office of Naval Research

1. A. J. Durelli, "Development of Experimental Stress Analysis Methods to Determine Stresses and Strains in Solid Propellant Grains"--June 1962. Developments in the manufacturing of grain-propellant models are reported. Two methods are given: a) cementing routed layers and b) casting.
2. A. J. Durelli and V. J. Parks, "New Method to Determine Restrained Shrinkage Stresses in Propellant Grain Models"--October 1962. The birefringence exhibited in the curing process of a partially restrained polyurethane rubber is used to determine the stress associated with restrained shrinkage in models of solid propellant grains partially bonded to the case.
3. A. J. Durelli, "Recent Advances in the Application of Photoelasticity in the Missile Industry"--October 1962. Two- and three-dimensional photoelastic analysis of grains loaded by pressure and by temperature are presented. Some applications to the optimization of fillet contours and to the redesign of case joints are also included.
4. A. J. Durelli and V. J. Parks, "Experimental Solution of Some Mixed Boundary Value Problems"--April 1964. Means of applying known displacements and known stresses to the boundaries of models used in experimental stress analysis are given. The application of some of these methods to the analysis of stresses in the field of solid propellant grains is illustrated. The presence of the "pinching effect" is discussed.
5. A. J. Durelli, "Brief Review of the State of the Art and Expected Advance in Experimental Stress and Strain Analysis of Solid Propellant Grains"--April 1964. A brief review is made of the state of the experimental stress and strain analysis of solid propellant grains. A discussion of the prospects for the next fifteen years is added.
6. A. J. Durelli, "Experimental Strain and Stress Analysis of Solid Propellant Rocket Motors"--March 1965. A review is made of the experimental methods used to strain-analyze solid propellant rocket motor shells and grains when subjected to different loading conditions. Methods directed at the determination of strains in actual rockets are included.
7. L. Ferrer, V. J. Parks and A. J. Durelli, "An Experimental Method to Analyze Gravitational Stresses in Two-Dimensional Problems"--October 1965. Photoelasticity and moiré methods are used to solve two-dimensional problems in which gravity-stresses are present.

8. A. J. Durelli, V. J. Parks and C. J. del Rio, "Stresses in a Square Slab Bonded on One Face to a Rigid Plate and Shrunk"--November 1965.
A square epoxy slab was bonded to a rigid plate on one of its faces in the process of curing. In the same process the photoelastic effects associated with a state of restrained shrinkage were "frozen-in." Three-dimensional photoelasticity was used in the analysis.
9. A. J. Durelli, V. J. Parks and C. J. del Rio, "Experimental Determination of Stresses and Displacements in Thick-Wall Cylinders of Complicated Shape"--April 1966.
Photoelasticity and moiré are used to analyze a three-dimensional rocket shape with a star shaped core subjected to internal pressure.
10. V. J. Parks, A. J. Durelli and L. Ferrer, "Gravitational Stresses Determined Using Immersion Techniques"--July 1966.
The methods presented in Technical Report No. 7 above are extended to three-dimensions. Immersion is used to increase response.
11. A. J. Durelli and V. J. Parks. "Experimental Stress Analysis of Loaded Boundaries in Two-Dimensional Second Boundary Value Problems"--February 1967.
The pinching effect that occurs in two-dimensional bonding problems, noted in Reports 2 and 4 above, is analyzed in some detail.
12. A. J. Durelli, V. J. Parks, H. C. Feng and F. Chiang, "Strains and Stresses in Matrices with Inserts,"-- May 1967.
Stresses and strains along the interfaces, and near the fiber ends, for different fiber end configurations, are studied in detail.
13. A. J. Durelli, V. J. Parks and S. Uribe, "Optimization of a Slot End Configuration in a Finite Plate Subjected to Uniformly Distributed Load,"--June 1967.
Two-dimensional photoelasticity was used to study various elliptical ends to a slot, and determine which would give the lowest stress concentration for a load normal to the slot length.
14. A. J. Durelli, V. J. Parks and Han-Chow Lee, "Stresses in a Split Cylinder Bonded to a Case and Subjected to Restrained Shrinkage,"--January 1968.
A three-dimensional photoelastic study that describes a method and shows results for the stresses on the free boundaries and at the bonded interface of a solid propellant rocket.
15. A. J. Durelli, "Experimental Stress Analysis Activities in Selected European Laboratories"--August 1968.
This report has been written following a trip conducted by the author through several European countries. A list is given of many of the laboratories doing important experimental stress analysis work and of the people interested in this kind of work. An attempt has been made to abstract the main characteristics of the methods used in some of the countries visited.

16. V. J. Parks, A. J. Durelli and L. Ferrer, "Constant Acceleration Stresses in a Composite Body"--October 1968.
Use of the immersion analogy to determine gravitational stresses in two-dimensional bodies made of materials with different properties.
17. A. J. Durelli, J. A. Clark and A. Kochev, "Experimental Analysis of High Frequency Stress Waves in a Ring"--October 1968.
A method for the complete experimental determination of dynamic stress distributions in a ring is demonstrated. Photoelastic data is supplemented by measurements with a capacitance gage used as a dynamic lateral extensometer.
18. J. A. Clark and A. J. Durelli, "A Modified Method of Holographic Interferometry for Static and Dynamic Photoelasticity"--April 1968.
A simplified absolute retardation approach to photoelastic analysis is described. Dynamic isopachics are presented.
19. J. A. Clark and A. J. Durelli, "Photoelastic Analysis of Flexural Waves in a Bar"--May 1969.
A complete direct, full-field optical determination of dynamic stress distribution is illustrated. The method is applied to the study of flexural waves propagating in a urethane rubber bar. Results are compared with approximate theories of flexural waves.
20. J. A. Clark and A. J. Durelli, "Optical Analysis of Vibrations in Continuous Media"--June 1969.
Optical methods of vibration analysis are described which are independent of assumptions associated with theories of wave propagation. Methods are illustrated with studies of transverse waves in prestressed bars, snap loading of bars and motion of a fluid surrounding a vibrating bar.
21. V. J. Parks, A. J. Durelli, K. Chandrashekara and T. L. Chen, "Stress Distribution Around a Circular Bar, with Flat and Spherical Ends, Embedded in a Matrix in a Triaxial Stress Field"--July 1969.
A Three-dimensional photoelastic method to determine stresses in composite materials is applied to this basic shape. The analyses of models with different loads are combined to obtain stresses for the triaxial cases.
22. A. J. Durelli, V. J. Parks and L. Ferrer, "Stresses in Solid and Hollow Spheres Subjected to Gravity or to Normal Surface Traction"--October 1969.
The method described in Report No. 10 above is applied to two specific problems. An approach is suggested to extend the solutions to a class of surface traction problems.
23. J. A. Clark and A. J. Durelli, "Separation of Additive and Subtractive Moiré Patterns"--December 1969.
A spatial filtering technique for adding and subtracting images of several gratings is described and employed to determine the whole field of Cartesian shears and rigid rotations.

24. R. J. Sanford and A. J. Durelli, "Interpretation of Fringes in Stress-Holo-Interferometry"--July 1970.
Errors associated with interpreting stress-holo-interferometry patterns as the superposition of isopachics (with half order fringe shifts) and isochromatics are analyzed theoretically and illustrated with computer generated holographic interference patterns.
25. J. A. Clark, A. J. Durelli and P. A. Laura, "On the Effect of Initial Stress on the Propagation of Flexural Waves in Elastic Rectangular Bars"--December 1970.
Experimental analysis of the propagation of flexural waves in prismatic, elastic bars with and without prestressing. The effects of prestressing by axial tension, axial compression and pure bending are illustrated.
26. A. J. Durelli and J. A. Clark, "Experimental Analysis of Stresses in a Buoy-Cable System Using a Birefringent Fluid"--February 1971.
An extension of the method of photoviscous analysis is presented which permits quantitative studies of strains associated with steady state vibrations of immersed structures. The method is applied in an investigation of one form of behavior of buoy-cable systems loaded by the action of surface waves.
27. A. J. Durelli and T. L. Chen, "Displacements and Finite-Strain Fields in a Sphere Subjected to Large Deformations"--February 1972.
Displacements and strains (ranging from 0.001 to 0.50) are determined in a polyurethane sphere subjected to several levels of diametral compression. A 500 lines-per-inch grating was embedded in a meridian plane of the sphere and moiré effect produced with a non-deformed master. The maximum applied vertical displacement reduced the diameter of the sphere by 27 per cent.
28. A. J. Durelli and S. Machida, "Stresses and Strain in a Disk with Variable Modulus of Elasticity"--March 1972
A transparent material with variable modulus of elasticity has been manufactured that exhibits good photoelastic properties and can also be strain analyzed by moiré. The results obtained suggests that the stress distribution in the disk of variable E is practically the same as the stress distribution in the homogeneous disk. It also indicates that the strain fields in both cases are very different, but that it is possible, approximately, to obtain the stress field from the strain field using the value of E at every point, and Hooke's law.
29. A. J. Durelli and J. Buitrago, "State of Stress and Strain in a Rectangular Belt Pulled Over a Cylindrical Pulley"--June 1972.
Two- and three-dimensional photoelasticity as well as electrical strain gages, dial gages and micrometers are used to determine the stress distribution in a belt-pulley system. Contact and tangential stress for various contact angles and friction coefficients are given.

30. T. L. Chen and A. J. Durelli, "Stress Field in a Sphere Subjected to Large Deformations"--June 1972.
Strain fields obtained in a sphere subjected to large diametral compressions from a previous paper were converted into stress fields using two approaches. First, the concept of strain-energy function for an isotropic elastic body was used. Then the stress field was determined with the Hookean type natural stress-natural strain relation. The results so obtained were also compared.
31. A. J. Durelli, V. J. Parks and H. M. Hasseem, "Helices Under Load"--July 1973.
Previous solutions for the case of close coiled helical springs and for helices made of thin bars are extended. The complete solution is presented in graphs for the use of designers. The theoretical development is correlated with experiments.
32. T. L. Chen and A. J. Durelli, "Displacements and Finite Strain Fields in a Hollow Sphere Subjected to Large Elastic Deformations"--September 1973.
The same methods described in No. 27, were applied to a hollow sphere with an inner diameter one half the outer diameter. The hollow sphere was loaded up to a strain of 30 per cent on the meridian plane and a reduction of the diameter by 20 per cent.
33. A. J. Durelli, H. H. Hasseem and V. J. Parks, "New Experimental Method in Three-Dimensional Elastostatics"--December 1973.
A new material is reported which is unique among three-dimensional stress-freezing materials, in that, in its heated (or rubbery) state it has a Poisson's ratio which is appreciably lower than 0.5. For a loaded model, made of this material, the unique property allows the direct determination of stresses from strain measurements taken at interior points in the model.
34. J. Wolak and V. J. Parks, "Evaluation of Large Strains in Industrial Applications"--April 1974.
It was shown that Mohr's circle permits the transformation of strain from one axis of reference to another, irrespective of the magnitude of the strain, and leads to the evaluation of the principal strain components from the measurement of direct strain in three directions.
35. A. J. Durelli, "Experimental Stress Analysis Activities in Selected European Laboratories"--April 1975.
Continuation of Report No. 15 after a visit to Belgium, Holland, Germany, France, Turkey, England and Scotland.
36. A. J. Durelli, V. J. Parks and J. O. Bühler-Vidal, "Linear and Non-linear Elastic and Plastic Strains in a Plate with a Big Hole Loaded Axially in its Plane"--July 1975.
Strain analysis of the ligament of a plate with a big hole indicates that both geometric and material non-linearity may take place. The strain concentration factor was found to vary from 1 to 2 depending on the level of deformation.

37. A. J. Durelli, V. Pavlin, J. O. Bühler-Vidal and G. Ome, "Elastostatics of a Cubic Box Subjected to Concentrated Loads"--August 1975.
Analysis of experimental strain, stress and deflection of a cubic box subjected to concentrated loads applied at the center of two opposite faces. The ratio between the inside span and the wall thickness was varied between approximately 5 and 121.
38. A. J. Durelli, V. J. Parks and J. O. Bühler-Vidal, "Elastostatics of Cubic Boxes Subjected to Pressure"--March 1976.
Experimental analysis of strain, stress and deflections in a cubic box subjected to either internal or external pressure. Inside span-to-wall thickness ratio varied from 5 to 14.
39. Y. Y. Hung, J. D. Hovanesian and A. J. Durelli, "New Optical Method to Determine Vibration-Induced Strains with Variable Sensitivity After Recording"--November 1976.
A steady state vibrating object is illuminated with coherent light and its image slightly misfocused. The resulting specklegram is "time-integrated" as when Fourier filtered gives derivatives of the vibrational amplitude.
40. Y. Y. Hung, C. Y. Liang, J. D. Hovanesian and A. J. Durelli, "Cyclic Stress Studies by Time-Averaged Photoelasticity"--November 1976.
"Time-averaged isochromatics" are formed when the photographic film is exposed for more than one period. Fringes represent amplitudes of the oscillating stress according to the zeroth order Bessel function.
41. Y. Y. Hung, C. Y. Liang, J. D. Hovanesian and A. J. Durelli, "Time-Averaged Shadow Moiré Method for Studying Vibrations"--November 1976.
Time-averaged shadow moiré permits the determination of the amplitude distribution of the deflection of a steady vibrating plate.
42. J. Buitrago and A. J. Durelli, "On the Interpretation of Shadow-Moiré Fringes"--April 1977.
Possible rotations and translations of the grating are considered in a general expression to interpret shadow-moiré fringes and on the sensitivity of the method. Application to an inverted perforated tube.
43. J. der Hovanesian, "18th Polish Solid Mechanics Conference." Published in European Scientific Notes of the Office of Naval Research, in London, England, Dec. 31, 1976.
Comments on the planning and organization of, and scientific content of paper presented at the 18th Polish Solid Mechanics Conference held in Wisla-Jawornik from September 7-14, 1976.
44. A. J. Durelli, "The Difficult Choice,"--May 1977.
The advantages and limitations of methods available for the analyses of displacements, strain, and stresses are considered. Comments are made on several theoretical approaches, in particular approximate methods, and attention is concentrated on experimental methods: photoelasticity, moiré, brittle and photoelastic coatings, gages, grids, holography and speckle to solve two- and three-dimensional problems in elasticity, plasticity, dynamics and anisotropy.

45. C. Y. Liang, Y. Y. Hung, A. J. Durelli and J. D. Hovanesian, "Direct Determination of Flexural Strains in Plates Using Projected Gratings,"--June 1977.
The method requires the rotation of one photograph of the deformed grating over a copy of itself. The moiré produced yields strains by optical double differentiation of deflections. Applied to projected gratings the idea permits the study of plates subjected to much larger deflections than the ones that can be studied with holograms.
46. A. J. Durelli, K. Brown and P. Yee, "Optimization of Geometric Discontinuities in Stress Fields"--March 1978.
The concept of "coefficient of efficiency" is introduced to evaluate the degree of optimization. An ideal design of the inside boundary of a tube subjected to diametral compression is developed which decreases its maximum stress by 25%, at the time it also decreases its weight by 10%. The efficiency coefficient is increased from 0.59 to 0.95. Tests with a brittle material show an increase in strength of 20%. An ideal design of the boundary of the hole in a plate subjected to axial load reduces the maximum stresses by 26% and increases the coefficient of efficiency from 0.54 to 0.90.
47. J. D. Hovanesian, Y. Y. Hung and A. J. Durelli, "New Optical Method to Determine Vibration-Induced Strains With Variable Sensitivity After Recording"--May 1978.
A steady-state vibrating object is illuminated with coherent light and its image is slightly misfocused in the film plane of a camera. The resulting processed film is called a "time-integrated specklegram." When the specklegram is Fourier filtered, it exhibits fringes depicting derivatives of the vibrational amplitude. The direction of the spatial derivative, as well as the fringe sensitivity may be easily and continuously varied during the Fourier filtering process. This new method is also much less demanding than holographic interferometry with respect to vibration isolation, optical set-up time, illuminating source coherence, required film resolution. etc.
48. Y. Y. Hung and A. J. Durelli, "Simultaneous Determination of Three Strain Components in Speckle Interferometry Using a Multiple Image Shearing Camera,"--September 1978
This paper describes a multiple image-shearing camera. Incorporating coherent light illumination, the camera serves as a multiple shearing speckle interferometer which measures the derivatives of surface displacements with respect to three directions simultaneously. The application of the camera to the study of flexural strains in bent plates is shown, and the determination of the complete state of two-dimensional strains is also considered. The multiple image-shearing camera uses an interference phenomena, but is less demanding than holographic interferometry with respect to vibration isolation and the coherence of the light source. It is superior to other speckle techniques in that the obtained fringes are of much better quality.

49. A. J. Durelli and K. Rajaiah, "Quasi-square Hole With Optimum Shape in an Infinite Plate Subjected to In-plane Loading"--January 1979. This paper deals with the optimization of the shape of the corners and sides of a square hole, located in a large plate and subjected to in-plane loads. Appreciable disagreement has been found between the results obtained previously by other investigators. Using an optimization technique, the authors have developed a quasi-square shape which introduces a stress concentration of only 2.54 in a uniaxial field, the comparable value for the circular hole being 3. The efficiency factor of the proposed optimum shape is 0.90, whereas the one of the best shape developed previously was 0.71. The shape also is developed that minimizes the stress concentration in the case of biaxial loading when the ratio of biaxiality is 1:-1.
50. A. J. Durelli and K. Rajaiah, "Optimum Hole Shapes in Finite Plates Under Uniaxial Load,"--February 1979. This paper presents optimized hole shapes in plates of finite width subjected to uniaxial load for a large range of hole to plate widths (D/W) ratios. The stress concentration factor for the optimized holes decreased by as much as 44% when compared to circular holes. Simultaneously, the area covered by the optimized hole increased by as much as 26% compared to the circular hole. Coefficients of efficiency between 0.91 and 0.96 are achieved. The geometries of the optimized holes for the D/W ratios considered are presented in a form suitable for use by designers. It is also suggested that the developed geometries may be applicable to cases of rectangular holes and to the tip of a crack. This information may be of interest in fracture mechanics.
51. A. J. Durelli and K. Rajaiah, "Determination of Strains in Photoelastic Coatings,"--May 1979. Photoelastic coatings can be cemented directly to actual structural components and tested under field conditions. This important advantage has made them relatively popular in industry. The information obtained, however, may be misinterpreted and lead to serious errors. A correct interpretation requires the separation of the principal strains and so far, this operation has been found very difficult. Following a previous paper by one of the authors, it is proposed to drill small holes in the coating and record the birefringence at points removed from the edge of the holes. The theoretical background of the method is reviewed; the technique necessary to use it is explained and two applications are described. The precision of the method is evaluated and found satisfactory in contradiction to information previously published in the literature.

52. A. J. Durelli and K. Rajaiah, "Optimized Inner Boundary Shapes in Circular Rings Under Diametral Compression,"--June 1979.
Using a method developed by the authors, the configuration of the inside boundary of circular rings, subjected to diametral compression, has been optimized, keeping cleared the space enclosed by the original circular inside boundary. The range of diameters studied was $0.33 \leq ID/OD \leq 0.7$. In comparison with circular rings of the same ID/OD, the stress concentrations have been reduced by about 30%, the weight has been reduced by about 10% and coefficients of efficiency of about 0.96 have been attained. The maximum values of compressive and tensile stresses on the edge of the hole, are approximately equal, there are practically no gradients of stress along the edge of the hole, and sharp corners exhibit zero stress. The geometries for each ID/OD design are given in detail.
53. A. J. Durelli and K. Rajaiah, "Lighter and Stronger,"--February 1980.
A new method has been developed that permits the direction design of shapes of two-dimensional structures and structural components, loaded in their plane, within specified design constraints and exhibiting optimum distribution of stresses. The method uses photoelasticity and requires a large field diffused light polariscope. Several problems of optimization related to the presence of holes in finite and infinite plates, subjected to uniaxial and biaxial loadings, are solved parametrically. Some unexpected results have been found: 1) the optimum shape of a large hole in a bar of finite width, subjected to uniaxial load, is "quasi" square, but the transverse boundary has the configuration of a "hat"; 2) for the small hole in the large plate, a "barrel" shape has a lower s.c.f. than the circular hole and appreciably higher coefficient of efficiency; 3) the optimum shape of a tube, subjected to diametral compression, has small "hinges" and is much lighter and stronger than the circular tube. Applications are also shown to the design of dove-tails and slots in turbine blades and rotors, and to the design of star-shaped solid propellant grains for rockets.

EXPERIMENTAL ANALYSIS OF DISPLACEMENTS AND SHEARS
AT THE SURFACE OF CONTACT BETWEEN TWO LOADED BODIES

by

C. Brémond and A. J. Durelli

ABSTRACT

The displacements which exist at the contact between two loaded bodies depend on the geometry of the surface of contact, the type of the loading and the property of the materials. A method has been developed to determine these displacements experimentally. A grid has been photographically printed on an interior plane of a transparent model of low modulus of elasticity. The displacements were recorded photographically and the analysis was conducted on the photographs of the deformed grids. Shears were determined from the change in angles. The precision of the measurements at the interface is estimated to be plus or minus 0.05mm. Examples of application are given for the cases of loads applied normally and tangentially to a rigid cylindrical punch resting on a semi-infinite soft plate. Important observations can be made on the zones of friction and of slip. The proposed method is three-dimensional and the distributions can be obtained at several interior planes by changing the position of the plane of the grid. The limitations of the method are pointed out. The possibility of using gratings (12 to 40 lpmm) is considered, as well as the advantages of using moiré to analyze the displacements.

EXPERIMENTAL ANALYSIS OF DISPLACEMENTS AND SHEARS
AT THE SURFACE OF CONTACT BETWEEN TWO LOADED BODIES

by

C. Brémond and A. J. Durelli

INTRODUCTION

It is very important to know the actual shear and normal stresses at the surface of contact between loaded bodies. The distribution of these stresses may determine the strength of the bodies, the wear of the surface and the damping of the vibrations.

Usually, theoretical approaches to the study of the distribution of stresses and strains at the surface of contact are conducted with one of the two following assumptions: a) there are only stresses normal to the surface (as in the Hertz problem)⁽¹⁾, or b) there is a pre-established relationship between the normal stress and the shear stress (Coulomb's law)^(2,3). Actually, in most structural problems, it is not possible to neglect, at the surface of contact, the value of the shear in respect to the normal stress⁽⁴⁾. Frequently, it is not correct either to fix the relationship between these two stresses⁽⁵⁾.

Attempts have been made to use finite element methods to solve this problem⁽⁶⁾. After the program has been developed, the determination is easy, but the method is essentially two-dimensional. It requires the use of a criterium of slip, and the values obtained are the average over the size of the elements.

Frequently, when these approaches are followed, displacement fields are determined as the result of the super-position of two solutions: 1) one

corresponding to a solid subjected to a concentrated force equivalent to the distributed applied force, and the other the solution corresponding to the semi-space subjected to the same load distributed over a finite area of the surface⁽⁷⁾. The problem is then divided in two but, in general, none of the solutions used is applicable to the total space considered⁽⁸⁾.

The experimental determination of these contact stresses is very difficult. It is almost impossible to locate gages on the loaded surfaces without changing the contact problem. Displacements to be measured are most of the times very small and frequently the state of stress is three-dimensional. In this paper, a three-dimensional grid method to measure displacement at the contact, using a model, is presented. From these displacements, shear strains and stresses can be determined. The method is also applicable everywhere in the field although in this case, it would be more practical to use the moiré effect. The results obtained for the contact of a cylinder resting on a plane show the existence of tangential displacements which are not negligible in comparison to the normal displacements and permit the analysis of the zones of friction and of slip at the contact.

CONSIDERATIONS ON THE OPTICAL METHODS

Two-dimensional photoelasticity is not well-suited, in general, to study the phenomenon of contact. The birefringence observed photoelastically is an effect integrated over all the points along the optical path. When the two bodies in contact are made of the same material, the distribution along the optical path may be three-dimensional, and this is even more so when the two bodies have been made from different materials.

The use of the three-dimensional "freezing" method of photoelasticity has also an important limitation. The materials in contact likely have different coefficients of thermal expansion. The freezing phenomena will be then associated not only with the mechanical effect but also with the thermal effect⁽⁹⁾. The scatter light method is not subjected to this limitation, but besides the much more difficult observation at the desired points and the less satisfactory sensitivity and precision, the resolution at the contact is not as good.

Moiré could be used for the study of the three-dimensional phenomena but is mainly useful for the exploration of the field. The displacements tangential to the contact change sign abruptly in the near vicinity of the contact.⁽⁷⁾ It would be necessary to use a grating of very high density and record fringes with very high resolution to obtain the necessary information at the contact.

In what follows, a particular way of using the grid will be described and an application will be presented.

ADVANTAGES OF THE GRID METHOD

The model to be used is transparent and made from a material of low modulus of elasticity. It is divided in two parts (Fig. 1) by the plane to be studied. On one of the two surfaces of the split model, a grid is printed and the two parts then are glued together. The grid is photographed after each level of load is applied to the model and the displacement is analyzed on the photograph of the deformed grid. Any plane can be chosen for the observation and, in this sense, the method is three-dimensional. The grid permits the observation of displacements taking place at points located very

near the surface of contact (of the order of $1/10\text{mm}$) which is much more difficult to do when photoelasticity is used mainly for the recording of isoclinics. The analysis has to be conducted point-by-point, which is time-consuming, but it is also true that isoclinics cannot be obtained but along isolated lines and that here also, the analysis is point-by-point.

Later, it will be shown that, in principle, the method could also use moiré effects for analysis if the grids are sufficiently dense and the resolution of the record sufficiently high. More details about embedded grids and embedded moiré can be found in other papers^{(10),(11),(12),(13)}.

DESCRIPTION OF THE MODEL

The transparent polyurethane rubber (photoflex), used to manufacture the models, has a modulus of elasticity $E = 0.3 \text{ daN/mm}^2$ and Poisson's ratio $\nu = 0.48$. The material is homogeneous and doesn't creep optically nor mechanically, after a few seconds of application of the load.

The grid is printed using a colored photosensitive emulsion which can be developed using Kodak P.E. 4125. This emulsion permitted the printing of grids with 2 and 12 lpmm, with good definition. To obtain good results, the model should be thoroughly washed, dried and cleaned with alcohol, then immersed in the emulsion and allowed to dry for 24 hours. The faces of the model, that have not been made photosensitive, are held in a frame. A master grid is put in contact with the photosensitized surface to print the grid using a 500 Watt lamp. The development requires only a few seconds and is done by contact with a cotton batting wetted in the developing solution. The surface is then washed with cold water. The model is finally finished by cementing to the printed surface the other

part of the model. Precaution should be taken to eliminate excessive glue and air bubbles at the interface. The model so manufactured consists of two parts of transparent rubber inbetween which there is a printed grid of cross-lines. The two faces of the interface are parallel and carefully machined (Fig. 1).

TESTS

The model is located in a beam of parallel light, and one of the machined faces is subjected to the action of the loaded cylinder. To obtain a good image of the plane of the grid, both the model and the cylinder are placed in a tank filled with a liquid which has the same index of refraction as the polyurethane used to manufacture the model. There is an appreciable deformation of the transverse cross-section of the model which would distort the path of light if the above described procedure is not used (Fig. 1).

It should be noted that the immersion in the liquid is associated with two restrictions. To keep the surface of contact dry, it is necessary to load the specimen before it is immersed in the liquid and therefore it is necessary to get the records for decreasing loads. It is also unfortunate that the liquid attacks the machined surfaces of the model and therefore the test cannot last more than about 10 minutes. This limitation, however, does not apply to the surface of contact which stays dry during the duration of the test.

The image of the model is received on a ground glass on which a scale in millimeters is printed. A first picture is taken before the model is loaded. A second picture is taken after the model is loaded and then the liquid is poured in the tank. Then each step of loading is recorded photographically.

ANALYSIS

Any enlargement of the records is made easier by the presence of the graph in millimeters which shows in the background of every photograph.

Every horizontal, as well as every vertical line of the grid, is identified by a number. Any point, located at the intersection of lines n and m , will be identified by the pair of numbers (n,m) . This pair corresponds to an abscissa x_n and an ordinate y_m in the system of reference xOy . A pair (n,m) of the grid has the position (x_n^0, y_m^0) in the nondeformed state (o), and the position (x_n^1, y_m^1) in the deformed state⁽¹⁾ (Fig. 2).

The components of displacement will then be given by

$$(u,v)^i_{(n,m)} = (x_n^0 - x_n^1, y_m^0 - y_m^1) \quad (1)$$

where u represents the tangential displacement in the direction Ox , v the displacement perpendicular in the direction Oy and i represents the level of the deformation. By using a graphical differentiation procedure⁽¹³⁾, the derivatives $\partial u/\partial x$ and $\partial v/\partial y$ can be obtained.

The component γ_{xy} is of particular interest and is proportional to the shear stress. In the plane of the grid

$$\gamma_{xy} = \frac{1}{2} (\partial u/\partial y + \partial v/\partial x) \text{ and } \sigma_{xy} = 2\mu\gamma_{xy} \quad (2)$$

Figure 3 shows the principle of the measurement. At the point $M(n,o)$ of the contact, two angles can be defined: a) angle θ_1 made by the tangent t_1 to the cylinder and the direction Ox ; b) angle θ_2 made by the direction Oy and the tangent t_2 to the line of the grid through point $M(n,o)$. The

measurement of each of these two angles permits the determination of the derivatives $\partial u/\partial y$ and $\partial v/\partial x$. From angles θ_1 and θ_2 in Fig. 3, measured in the positive direction, it follows:

$$\tan\theta_1 = \partial v/\partial x \text{ and } \tan\theta_2 = -\partial u/\partial y \quad (3)$$

from which the value of γ_{xy} can be obtained:

$$2\gamma_{xy} = \tan\theta_1 - \tan\theta_2 \quad (4)$$

Actually, to obtain a good precision, it is necessary to read the angle θ_2 several times. The sign of γ_{xy} can be obtained directly by comparing the angle (t_1, t_2) to $\pi/2$.

RESULTS

The tests reported here were conducted on a model on which the printed grid had two lines per mm. The dimensions of the model were 26 x 100 x 120 mm. The cylindrical punch was made of plexiglass and had a diameter of 40 mm. The contact was obtained when the surface was dry and the load was 200 N. This situation corresponds to the test identified as one. The other four tests were obtained at different levels of load.

Displacements at the Surface of the Model

In Fig. 4, the normal displacement v and the tangential displacement u of point (n,o) of the grid, located at the surface of the model, have been represented. The center of the contact was observed at the beginning of the tests and takes place at (46.0).

The normal displacement v which is perfectly symmetric with respect to the center of contact for the tests of normal load, is not symmetric

any more when the tangential load increases (test 5): that is how displacement v at points (31.0) and (55.0), which correspond respectively to the edges ($-a$ and $+a$) of the contact, are no more symmetric with respect to the new center of contact taking place at the point (45.0).

Tangential displacement u takes place towards the center of contact and is antisymmetric for the tests conducted under normal load. Recalling that the tangential displacement at the contact is smaller, when Poisson's ratio is larger, as shown by Poritsky⁽⁷⁾, the results obtained indicate that, at the contact, the tangential displacements due to a normal load are not negligible with respect to the normal displacements. This has been found even for the conditions of the test for which $\nu = 0.48$. In test 1, v varies between -3 and -1.7 mm and u varies from 0 to 0.4 mm. These results show that, if it is true that the influence of the tangential load on the normal displacement is small and has, as a consequence, mainly an assymetry of the contact, to neglect the influence of the normal load on the tangential displacements may lead to non-negligible errors.

Zones of Adherence and Zones of Slip at the Contact

From the examination of the successive tangential displacements of points located at the contact, it is possible to follow the evolution of the zones of adherence and the zones of slip. For tests 1, 2 and 3, conducted under normal load, the zone of adherence (44.0) (46.0) (48.0) stays constant at the center of contact and the zone of slip varies on both sides depending on the length of contact. On the other hand, for tests 4 and 5, conducted under tangential loads, the zone of adherence decreases in length and moves toward $x > 0$ at the same time that the slip increases ahead of the contact.

Shears at the Surface of Contact

Figure 5 represents the results obtained for $\partial v/\partial x$, $\partial u/\partial y$ and σ_{xy}/μ for the five tests.

Under normal load, the curve representing σ_{xy}/μ is antisymmetric and indicates that the shear stresses are directed towards the outside of the contact and reach a maximum near the edge of the contact. Under oblique load, the shear stresses are opposite to the applied tangential force and the shape of the curve obtained from test 5 is the shape of the distribution obtained by Carter⁽¹⁴⁾.

In test 2, a decrease of the normal load brings an increase of σ_{xy} . In test 3, an increase of the normal load brings a change in the sign of the shear stresses in the zone which becomes again a zone of contact, there where the liquid has penetrated.

PRECISION OF THE RESULTS

The analysis of the displacements has been conducted on graph paper with readings estimated at $\pm 0.25\text{mm}$. The precision corresponding to the model is estimated to be 0.05mm . It is possible, therefore, to estimate $1/10$ of the maximum amplitude of the tangential displacement. For the graphical determination of σ_{xy} , the angles θ_1 and θ_2 are measured with the reproducibility of 1° which corresponds to an error of $1/30$ for $2\gamma_{xy}$. Only curves of tests 2, 4 and 5 give significant amplitudes.

LIMITATION OF THE METHOD

The tangential displacement u is directed towards the center of the surface of contact and changes sign in the immediate neighborhood of the

surface of contact^{(7),(15)}. The gradient of this displacement is steep and the method of the grid is particularly well adapted to the measurement of displacements in this region. However, a point-by-point determination, in the rest of the field, is time-consuming. The analysis would be easier if denser grids can be used and advantage be taken of moiré effects. Tests with 12 lpmm permit a good evaluation of the displacements perpendicular to the surface of contact, but not of those tangential to it. Tests by Kawatate do not seem to have better resolution than 0.5mm, with 20 lpmm gratings⁽¹⁶⁾. In a previous paper, one of the authors used 20 lpmm on the meridian plane of a sphere⁽¹²⁾. The contact zone was not of interest at that time, but the resolution does not seem to be better than the one obtained in this paper. It was not possible then to photograph gratings with 40 lpmm. For completeness, it should be mentioned that some attempts have been made to use electrical resistance strain gages to determine the strains at the contact; see for instance⁽¹⁷⁾. The base length of these gages, however, is of the order of 2mm.

The materials used in the tests deformed appreciably, but the mechanical behavior was linear within the range of the deformations imposed. Poisson's ratio was close to .5 and the conclusions obtained cannot be applied without further thought to the contact between harder materials. Finally, the requirement of immersing the model in the liquid doesn't permit the observation of the displacement under increasing load.

CONCLUSION

An experimental method has been developed that permits the measurement of three-dimensional displacements and shear angles at the surface of contact between two loaded bodies. The method has been applied to the solution of

the problem of the cylindrical punch in contact with a semi-infinite plate. The study shows that the displacements tangential to the surface of contact are not negligible with respect to the displacements perpendicular to that surface, and that the method used permits estimation of their maximum amplitude $\pm 1/10$ of this amplitude. The study shows also the zones of adherence and of slip at the contact. In a future paper, a method to determine directly the stresses normal and tangential to the contact, from the measured displacements, will be presented.

ACKNOWLEDGMENTS

The research program from which this paper was developed was supported in part by the Office of Naval Research (Contract No. N0014-76-C-0487). The authors are grateful to N. Perrone and N. Basdekas of ONR for their support. The manuscript reproduction has been prepared by P. Baxter.

REFERENCES

1. Hertz H., "Ueber die Berührung Fester Elastischer Körper", J. für Math., Vol. 92, pp. 156-171, 1882.
2. Carter F. W., "On the Action of a Locomotive Driving Wheel", Proc. Roy. Soc., Series A, Vol. 112, pp. 151-157, 1926.
3. Cattaneo C., "Sul Contatto di due Corpi Elastici: Distribuzione Locale Degli Sforzi", Rend. Acad. Lincei, Series 6, Vol. 27, pp. 342-348, 434-436, 474-478, 1938.
4. Johnson K. L., "A Review of the Theory of Rolling Contact Stresses", Wear, Vol. 9, pp. 4-19, 1966.
5. Spence D. A., "An Eigenvalue Problem for Elastic Contact With Finite Friction", Proc. Camb. Phil. Soc., Vol. 73, pp. 249-268, 1973.
6. Gaertner R., "Investigation of Plane Elastic Contact Allowing for Friction", Comp. Structures, Vol. 7, pp. 59-63, 1977.
7. Poritsky H., "Stresses and Deflections of Cylindrical Bodies in Contact With Application etc.", J. Appl. Mech., Vol. 17, pp. 191-201, 1950.
8. Schwartz J. and Harper E. Y., "On the Relative Approach of Two-dimensional Elastic Bodies in Contact", Int. J. Sol. Struc., Vol. 7, pp. 1613-1626, 1971.
9. Durelli A. J. and Riley W. F., "Introduction of Photomechanics", Prentice-Hall, 1965.
10. Durelli A. J. and Daniel I., "A Non-destructive Three-dimensional Strain Analysis Method", J. App. Mech., Vol. 28, E, No. 1, pp. 83-86. March 1961.
11. Durelli A. J. and Chen T. L., "Displacement and Finite-strain Fields in a Sphere Subjected to Large Deformations", Int. J. Non-lin. Mech. Sci., Vol. 8, pp. 17-30, 1973.

12. Chen T. L. and Durelli A. J., "Displacements and Finite-strain Fields in a Hollow Sphere Subjected to Large Deformations", Int. J. Non-lin. Mech. Sci., Vol. 16, pp. 777-788, 1974.
13. Durelli A. J., "Applied Stress Analysis", Prentice-Hall, 1967.
14. Carter F. W., "On the Action of Locomotive Driving Wheel", Proc. Roy. Soc., Series A, Vol. 112, p. 151, 1926.
15. Brémond C., "Résolution du Problème de Contact Élastique Plan Avec Frottement à Partir de Données Expérimentales", Thèse Dr. Ing., Univ. Lyon, 1976.
16. Kawatate K., "Transition of Collision Contact Force Between a Visco Elastic Half-space and a Flat-headed Rigid Body", Proc. JNCAM, pp. 441-452, 1975.
17. Rumelhart C., Martineau G. and Bahuaud J., "Etude de la Répartition des Pressions à la Surface d'un Modèle de Prothèse Totale de Hanche de Type MC Kec-Farrar", Proc. Fifth Int. Conf. Exp. St. An. Udine, pp. 3.70 - 3.79, 1974.

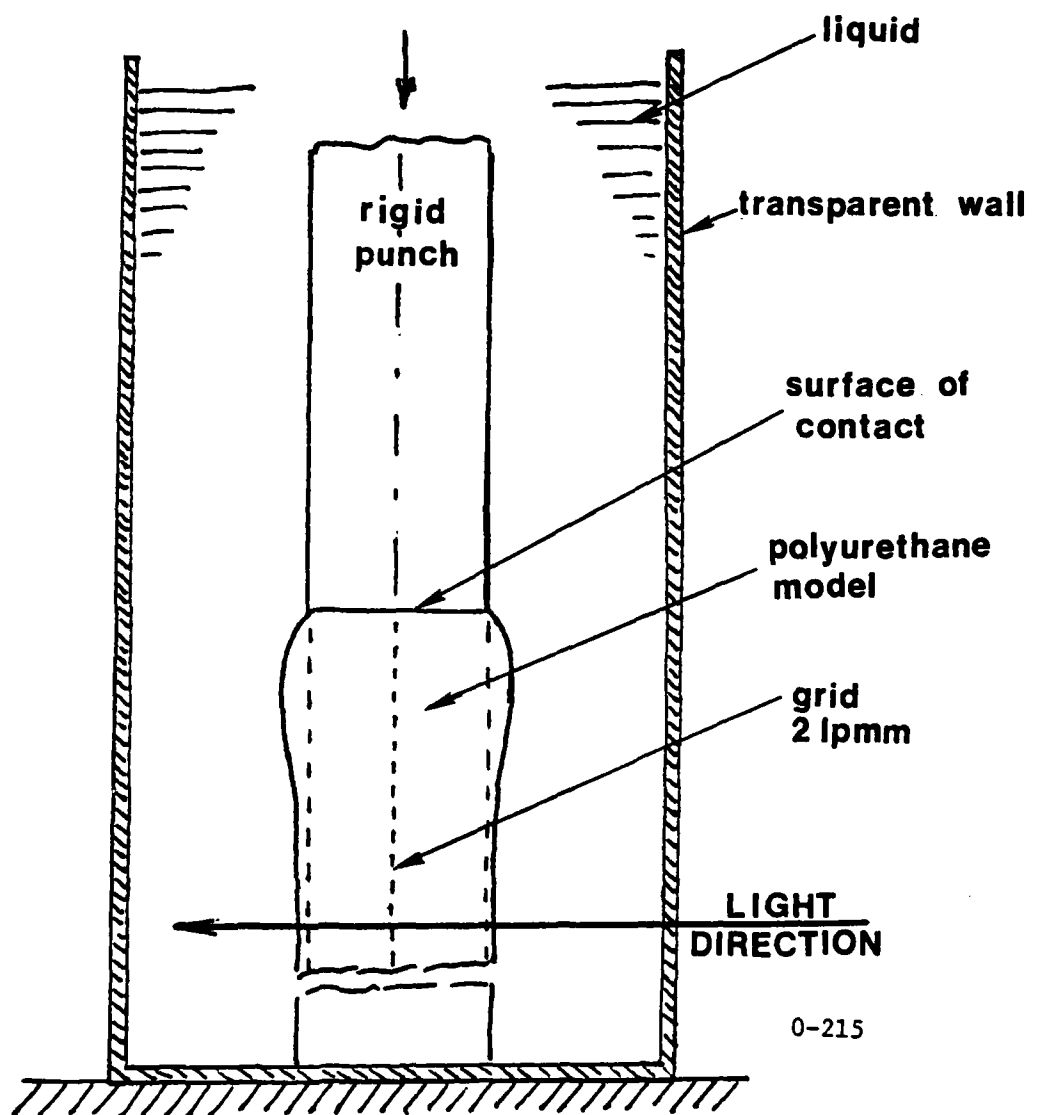


FIGURE 1 TRANSVERSE CROSS-SECTION OF MODEL AND LOADING SET-UP.

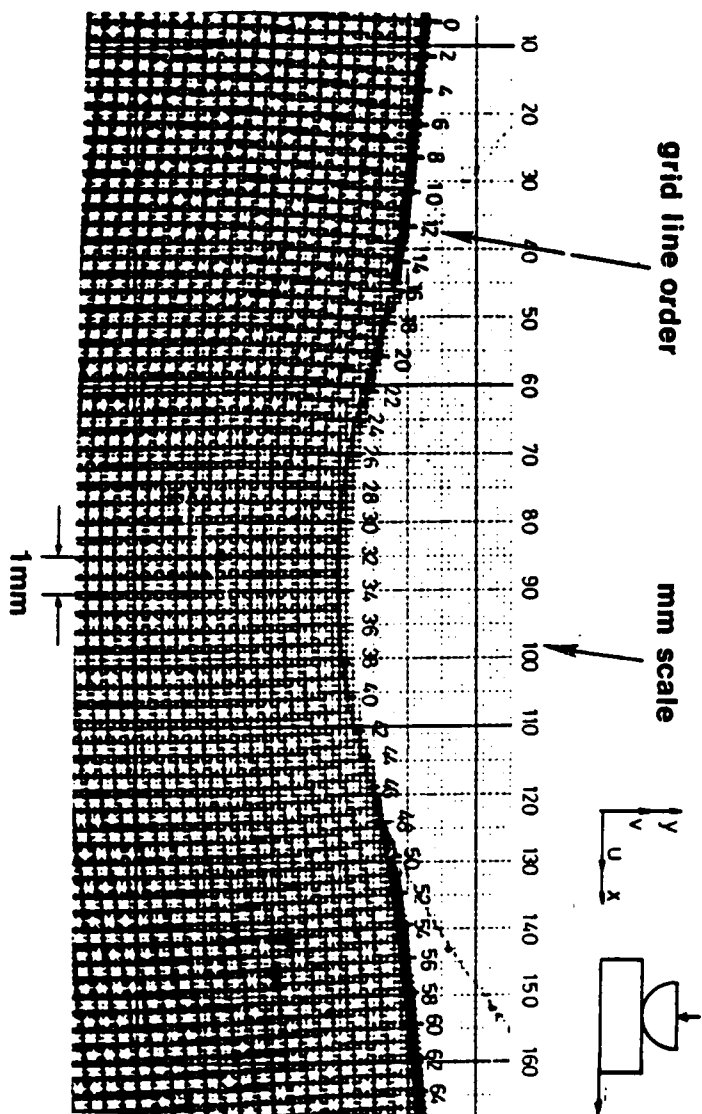
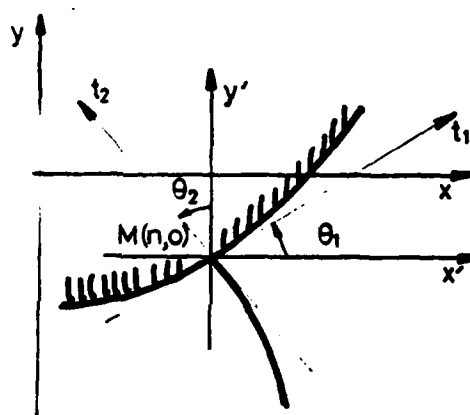
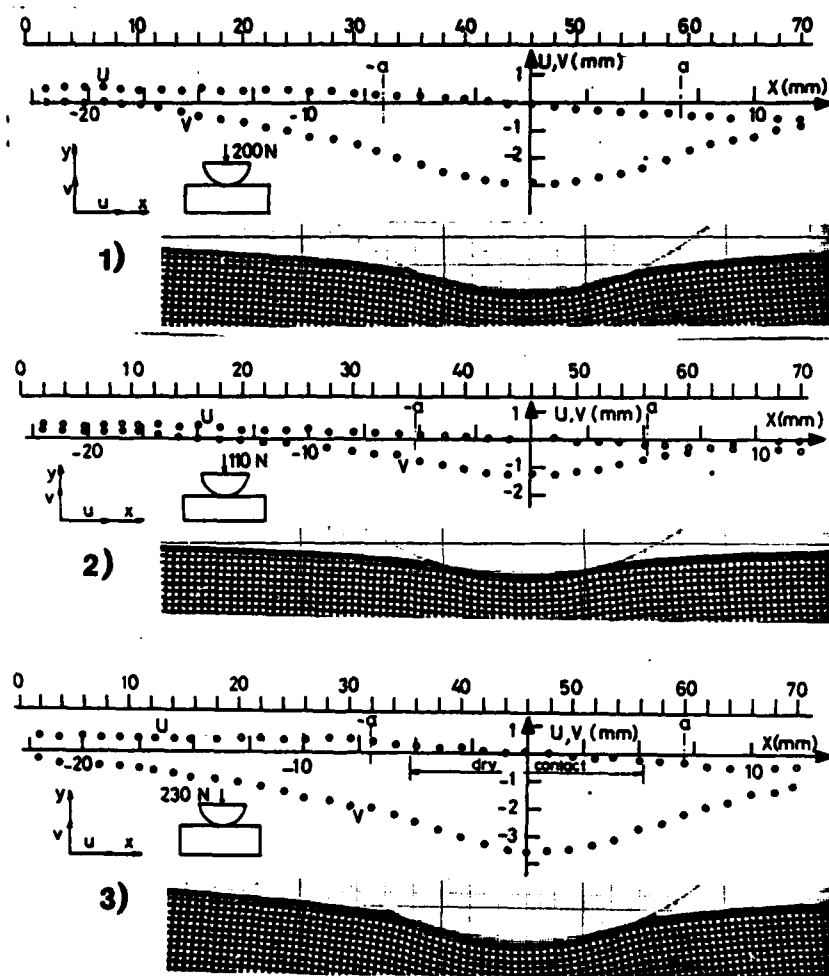


FIG. 2 IMAGE OF THE DEFORMED GRID AND THE REFERENCE SCALE IN MILLIMETERS.



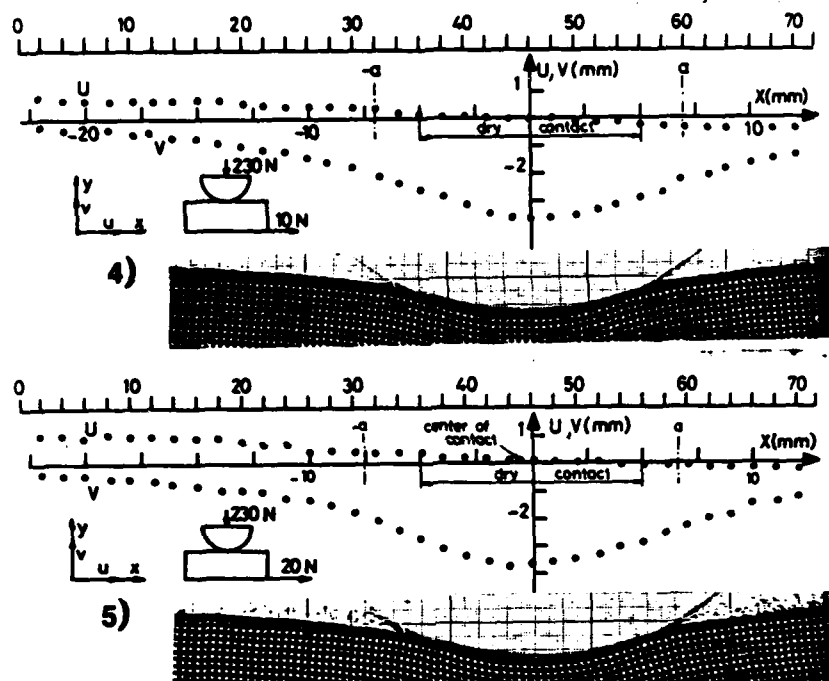
0-216

FIG. 3 ANGULAR MEASUREMENTS TO DETERMINE THE STRAIN



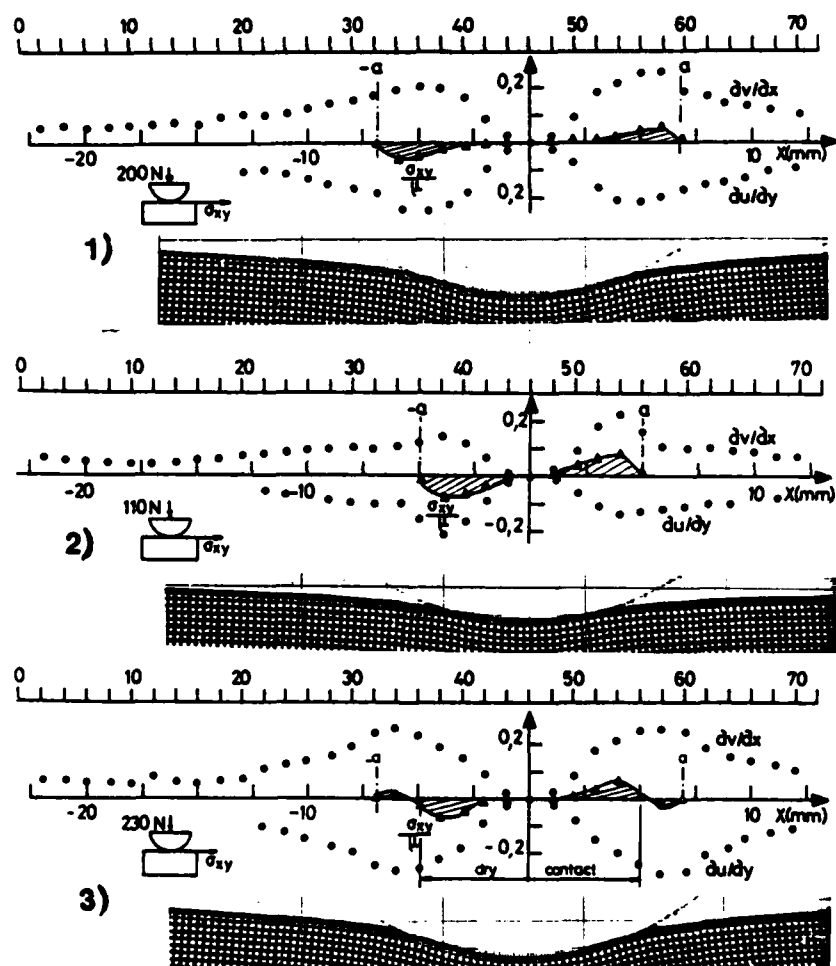
0-217

FIG. 4a DISPLACEMENTS U AND V AT THE SURFACE OF CONTACT BETWEEN A CYLINDRICAL PUNCH AND A SEMI-SPACE (LOAD PERPENDICULAR TO THE INTERFACE).



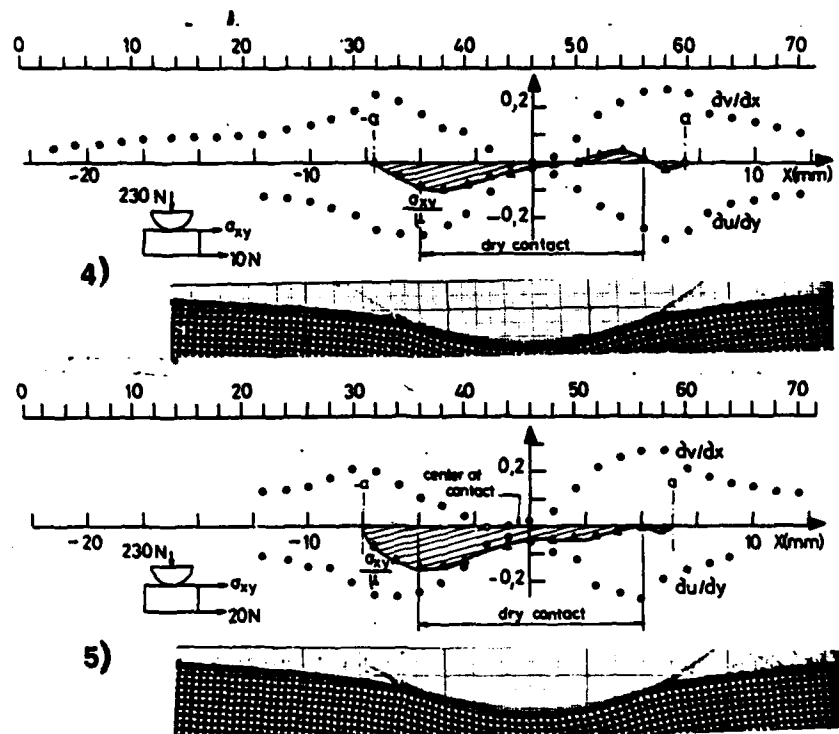
0-218

FIG. 4b DISPLACEMENTS u AND v AT THE SURFACE OF CONTACT BETWEEN A CYLINDRICAL PUNCH AND A SEMI-SPACE (LOAD OBLIQUE TO THE INTERFACE).



0-219

FIG. 5a SHEAR STRAINS AT THE SURFACE OF CONTACT BETWEEN A CYLINDRICAL PUNCH AND A SEMI-SPACE (LOAD PERPENDICULAR TO THE INTERFACE).



0-220

FIG. 5b SHEAR STRAINS AT THE SURFACE OF CONTACT BETWEEN A CYLINDRICAL PUNCH AND A SEMI-SPACE (LOAD OBLIQUE TO THE INTERFACE).

ONR DISTRIBUTION LIST

Part 1 - Government Administrative and Liaison Activities

Office of Naval Research
Department of the Navy
Arlington, Virginia 22217
Attn: Code 474 (2)
Code 471
Code 200

Director
Office of Naval Research
Branch Office
666 Summer Street
Boston, Massachusetts 02210

Director
Office of Naval Research
Branch Office
536 South Clark Street
Chicago, Illinois 60605

Director
Office of Naval Research
New York Area Office
715 Broadway - 5th Floor
New York, New York 10003

Director
Office of Naval Research
Branch Office
1030 East Green Street
Pasadena, California 91106

Naval Research Laboratory (6)
Code 2627
Washington, D.C. 20375

Defense Documentation Center (12)
Cameron Station
Alexandria, Virginia 22314

Navy

Undersea Explosion Research Division
Naval Ship Research and Development
Center

Norfolk Naval Shipyard
Portsmouth, Virginia 23709
Attn: Dr. E. Palmer, Code 177

Naval Research Laboratory
Washington, D.C. 20375
Attn: Code 8400
8410
8430
8440
6300
6390
6380

David W. Taylor Naval Ship Research
and Development Center
Annapolis, Maryland 21402
Attn: Code 2740
28
281

Naval Weapons Center
China Lake, California 93555
Attn: Code 4062
4520

Commanding Officer
Naval Civil Engineering Laboratory
Code L31
Port Hueneme, California 93041

Naval Surface Weapons Center
White Oak
Silver Spring, Maryland 20910
Attn: Code R-10
G-402
K-82

Technical Director
Naval Ocean Systems Center
San Diego, California 92152

Navy (Con't.)

Supervisor of Shipbuilding
U.S. Navy
Newport News, Virginia 23607

Navy Underwater Sound
Reference Division
Naval Research Laboratory
P.O. Box 8337
Orlando, Florida 32806

Chief of Naval Operations
Department of the Navy
Washington, D.C. 20350
Attn: Code OP-098

Strategic Systems Project Office
Department of the Navy
Washington, D.C. 20376
Attn: NSP-200

Naval Air Systems Command
Department of the Navy
Washington, D.C. 20361
Attn: Code 5302 (Aerospace and Structures)
604 (Technical Library)
320B (Structures)

Naval Air Development Center
Warminster, Pennsylvania 18974
Attn: Aerospace Mechanics
Code 606

U.S. Naval Academy
Engineering Department
Annapolis, Maryland 21402

Naval Facilities Engineering Command
200 Stovall Street
Alexandria, Virginia 22332
Attn: Code 03 (Research and Development)
04B
04S
14114 (Technical Library)

Naval Sea Systems Command
Department of the Navy
Washington, D.C. 20362
Attn: Code 05H
312
322
323
05R
32R

Commander and Director
David W. Taylor Naval Ship
Research and Development Center
Bethesda, Maryland 20084
Attn: Code 042
17
172
173
174
1800
1844
012.2
1900
1901
1945
1960
1962

Naval Underwater Systems Center
Newport, Rhode Island 02840
Attn: Dr. R. Trainor

Naval Surface Weapons Center
Dahlgren Laboratory
Dahlgren, Virginia 22448
Attn: Code G04
G20

Technical Director
Mare Island Naval Shipyard
Vallejo, California 94592

Navy (Con't.)

U.S. Naval Postgraduate School
Library
Code 0384
Monterey, California 93940

Webb Institute of Naval Architecture
Attn: Librarian
Crescent Beach Road, Glen Cove
Long Island, New York 11542

ARMY

Commanding Officer (2)
U.S. Army Research Office
P.O. Box 12211
Research Triangle Park, NC 27709
Attn: Mr. J. J. Murray, CRD-AA-IP

Watervliet Arsenal
MAGGS Research Center
Watervliet, New York 12189
Attn: Director of Research

U.S. Army Materials and Mechanics
Research Center
Watertown, Massachusetts 02172
Attn: Dr. R. Shea, DRMR-T

U.S. Army Missile Research and
Development Center
Redstone Scientific Information
Center
Chief, Document Section
Redstone Arsenal, Alabama 35809

Army Research and Development
Center
Fort Belvoir, Virginia 22060

NASA

National Aeronautics and Space
Administration
Structures Research Division
Langley Research Center
Langley Station
Hampton, Virginia 23365

National Aeronautics and Space
Administration
Associate Administrator for Advanced
Research and Technology
Washington, D.C. 20546

Air Force

Wright-Patterson Air Force Base
Dayton, Ohio 45433
Attn: AFFDL (FB)
(FBR)
(FBE)
(FBS)
AFML (MEM)

Chief Applied Mechanics Group
U.S. Air Force Institute of Technology
Wright-Patterson Air Force Base
Dayton, Ohio 45433

Chief, Civil Engineering Branch
WLRC, Research Division
Air Force Weapons Laboratory
Kirtland Air Force Base
Albuquerque, New Mexico 87117

Air Force Office of Scientific Research
Bolling Air Force Base
Washington, D.C. 20332
Attn: Mechanics Division

Department of the Air Force
Air University Library
Maxwell Air Force Base
Montgomery, Alabama 36112

Other Government Activities

Commandant
Chief, Testing and Development Division
U.S. Coast Guard
1300 E Street, NW.
Washington, D.C. 20226

Technical Director
Marine Corps Development
and Education Command
Quantico, Virginia 22134

Director Defense Research
and Engineering
Technical Library
Room 3C128
The Pentagon
Washington, D.C. 20301

Dr. M. Gaus
National Science Foundation
Environmental Research Division
Washington, D.C. 20550

Library of Congress
Science and Technology Division
Washington, D.C. 20540

Director
Defense Nuclear Agency
Washington, D.C. 20305
Attn: SPSS

Mr. Jerome Persh
Staff Specialist for Materials
and Structures
OUSD&E, The Pentagon
Room 3D1089
Washington, D.C. 20301

Chief, Airframe and Equipment Branch
FS-120
Office of Flight Standards
Federal Aviation Agency
Washington, D.C. 20553

National Academy of Sciences
National Research Council
Ship Hull Research Committee
2101 Constitution Avenue
Washington, D.C. 20418
Attn: Mr. A. R. Lytle

National Science Foundation
Engineering Mechanics Section
Division of Engineering
Washington, D.C. 20550

Picatinny Arsenal
Plastics Technical Evaluation Center
Attn: Technical Information Section
Dover, New Jersey 07801

Maritime Administration
Office of Maritime Technology
14th and Constitution Avenue, NW.
Washington, D.C. 20230

Universities

Dr. J. Tinsley Oden
University of Texas at Austin
345 Engineering Science Building
Austin, Texas 78712

Professor Julius Miklowitz
California Institute of Technology
Division of Engineering
and Applied Sciences
Pasadena, California 91109

Dr. Harold Liebowitz, Dean
School of Engineering and
Applied Science
George Washington University
Washington, D.C. 20052

Professor Eli Sternberg
California Institute of Technology
Division of Engineering and
Applied Sciences
Pasadena, California 91109

Professor Paul M. Naghdí
University of California
Department of Mechanical Engineering
Berkeley, California 94720

Professor A. J. Durallí
Oakland University
School of Engineering
Rochester, Missouri 48063

Professor F. L. DiMaggio
Columbia University
Department of Civil Engineering
New York, New York 10027

Professor Norman Jones
The University of Liverpool
Department of Mechanical Engineering
P. O. Box 147
Brownlow Hill
Liverpool L69 3BX
England

Professor E. J. Skudrzyk
Pennsylvania State University
Applied Research Laboratory
Department of Physics
State College, Pennsylvania 16801

Professor J. Klosner
Polytechnic Institute of New York
Department of Mechanical and
Aerospace Engineering
333 Jay Street
Brooklyn, New York 11201

Professor R. A. Schapery
Texas A&M University
Department of Civil Engineering
College Station, Texas 77843

Professor Walter D. Pilkey
University of Virginia
Research Laboratories for the
Engineering Sciences and
Applied Sciences
Charlottesville, Virginia 22901

Professor K. D. Willmert
Clarkson College of Technology
Department of Mechanical Engineering
Potdam, New York 13676

Professor R. S. Rivlin
Lehigh University
Center for the Application
of Mathematics
Bethlehem, Pennsylvania 18015

Universities (Con't)

Dr. Walter E. Haider
Texas A&M University
Aerospace Engineering Department
College Station, Texas 77843

Dr. Hussein A. Kamal
University of Arizona
Department of Aerospace and
Mechanical Engineering
Tucson, Arizona 85721

Dr. S. J. Farnes
Carnegie-Mellon University
Department of Civil Engineering
Schenley Park
Pittsburgh, Pennsylvania 15213

Dr. Ronald L. Huston
Department of Engineering Analysis
University of Cincinnati
Cincinnati, Ohio 45221

Professor G. C. M. Sih
Lehigh University
Institute of Fracture and
Solid Mechanics
Bethlehem, Pennsylvania 18015

Professor Albert S. Kobayashi
University of Washington
Department of Mechanical Engineering
Seattle, Washington 98105

Professor Daniel Frederick
Virginia Polytechnic Institute and
State University
Department of Engineering Mechanics
Blacksburg, Virginia 24061

Professor A. C. Eringen
Princeton University
Department of Aerospace and
Mechanical Sciences
Princeton, New Jersey 08540

Professor E. H. Lee
Stanford University
Division of Engineering Mechanics
Stanford, California 94305

Professor Albert I. King
Wayne State University
Biomechanics Research Center
Detroit, Michigan 48202

Dr. V. R. Hodgson
Wayne State University
School of Medicine
Detroit, Michigan 48202

Dean B. A. Boley
Northwestern University
Department of Civil Engineering
Evanston, Illinois 60201

Professor H. W. Liu
Syracuse University
Department of Chemical Engineering
and Metallurgy
Syracuse, New York 13210

Professor S. Bodner
Technion R&D Foundation
Haifa, Israel

Professor Werner Goldsmith
University of California
Department of Mechanical Engineering
Berkeley, California 94720

Universities (Con't)

Professor P. G. Hodge, Jr.
University of Minnesota
Department of Aerospace Engineering
and Mechanics
Minneapolis, Minnesota 55455

Dr. B. C. Drucker
University of Illinois
Dean of Engineering
Urbana, Illinois 61801

Professor H. M. Newmark
University of Illinois
Department of Civil Engineering
Urbana, Illinois 61803

Professor E. Raisener
University of California, San Diego
Department of Applied Mechanics
La Jolla, California 92037

Professor William A. Nash
University of Massachusetts
Department of Mechanics and
Aerospace Engineering
Amherst, Massachusetts 01002

Professor G. Herrmann
Stanford University
Department of Applied Mechanics
Stanford, California 94305

Professor J. D. Achenbach
Northwest University
Department of Civil Engineering
Evanston, Illinois 60201

Professor S. B. Dong
University of California
Department of Mechanics
Los Angeles, California 90024

Professor Burt Paul
University of Pennsylvania
Towne School of Civil and
Mechanical Engineering
Philadelphia, Pennsylvania 19104

Professor F. A. Cozzarelli
State University of New York at
Buffalo
Division of Interdisciplinary Studies
Karr Parker Engineering Building
Chemistry Road
Buffalo, New York 14214

Professor Joseph L. Rose
Drexel University
Department of Mechanical Engineering
and Mechanics
Philadelphia, Pennsylvania 19104

Professor B. K. Donaldson
University of Maryland
Aerospace Engineering Department
College Park, Maryland 20742

Professor Joseph A. Clark
Catholic University of America
Department of Mechanical Engineering
Washington, D.C. 20064

Dr. Samuel S. Batdorf
University of California
School of Engineering
and Applied Science
Los Angeles, California 90024

Professor Isaac Fried
Boston University
Department of Mathematics
Boston, Massachusetts 02215

Universities (Con't)

Professor E. Krampl
Rensselaer Polytechnic Institute
Division of Engineering
Engineering Mechanics
Troy, New York 12181

Dr. Jack R. Vinson
University of Delaware
Department of Mechanical and Aerospace
Engineering and the Center for
Composite Materials
Newark, Delaware 19711

Dr. J. Duffy
Brown University
Division of Engineering
Providence, Rhode Island 02912

Dr. J. L. Szwedlow
Carnegie-Mellon University
Department of Mechanical Engineering
Pittsburgh, Pennsylvania 15213

Dr. V. K. Varadan
Ohio State University Research Foundation
Department of Engineering Mechanics
Columbus, Ohio 43210

Dr. Z. Hashin
University of Pennsylvania
Department of Metallurgy and
Materials Science
College of Engineering and
Applied Science
Philadelphia, Pennsylvania 19104

Dr. Jackson C. S. Yang
University of Maryland
Department of Mechanical Engineering
College Park, Maryland 20742

Professor T. Y. Chang
University of Akron
Department of Civil Engineering
Akron, Ohio 44325

Professor Charles W. Bert
University of Oklahoma
School of Aerospace, Mechanical,
and Nuclear Engineering
Norman, Oklahoma 73019

Professor Satya N. Atluri
Georgia Institute of Technology
School of Engineering and
Mechanics
Atlanta, Georgia 30332

Professor Graham F. Carey
University of Texas at Austin
Department of Aerospace Engineering
and Engineering Mechanics
Austin, Texas 78712

Dr. S. S. Wang
University of Illinois
Department of Theoretical and
Applied Mechanics
Urbana, Illinois 61801

Industry and Research Institutes

Dr. Norman Hobbs
Kaman Avidyne
Division of Kaman
Sciences Corporation
Burlington, Massachusetts 01803

Argonne National Laboratory
Library Services Department
9700 South Cass Avenue
Argonne, Illinois 60440

Industry and Research Institutes (Con't)

Dr. M. C. Junger
Cambridge Acoustical Associates
54 Rindge Avenue Extension
Cambridge, Massachusetts 02140

Dr. V. Codino
General Dynamics Corporation
Electric Boat Division
Groton, Connecticut 06340

Dr. J. E. Greenspan
J. G. Engineering Research Associates
3831 Menlo Drive
Baltimore, Maryland 21215

Newport News Shipbuilding and
Dry Dock Company
Library
Newport News, Virginia 23607

Dr. W. F. Bozich
McDonnell Douglas Corporation
5301 Bolsa Avenue
Huntington Beach, California 92647

Dr. H. N. Abramson
Southwest Research Institute
8500 Culebra Road
San Antonio, Texas 78284

Dr. R. C. DeHart
Southwest Research Institute
8500 Culebra Road
San Antonio, Texas 78284

Dr. M. L. Baron
Weidinger Associates
110 East 59th Street
New York, New York 10022

Dr. T. L. Geers
Lockheed Missiles and Space Company
3251 Hanover Street
Palo Alto, California 94304

Mr. William Caywood
Applied Physics Laboratory
Johns Hopkins Road
Laurel, Maryland 20810

Dr. Robert E. Dunham
Pacifica Technology
P.O. Box 148
Del Mar, California 92014

Dr. M. F. Kanninen
Battelle Columbus Laboratories
505 King Avenue
Columbus, Ohio 43201

Dr. A. A. Hochrein
Daedalean Associates, Inc.
Springlake Research Road
15110 Frederick Road
Woodbine, Maryland 21797

Dr. James W. Jones
Swanson Service Corporation
P.O. Box 5415
Huntington Beach, California 92646

Dr. Robert E. Nickell
Applied Science and Technology
3344 North Torrey Pines Court
Suite 220
La Jolla, California 92037

Dr. Kevin Thomas
Westinghouse Electric Corp.
Advanced Reactors Division
P. O. Box 158
Madison, Pennsylvania 15663

REPORT DOCUMENTATION PAGE		READ INSTRUCTIONS BEFORE COMPLETING FORM
1. REPORT NUMBER 54	2. GOVT ACCESSION NO. AD-A086949	3. RECIPIENT'S CATALOG NUMBER
4. TITLE (and Subtitle) EXPERIMENTAL ANALYSIS OF DISPLACEMENTS AND SHEARS AT THE SURFACE OF CONTACT BETWEEN TWO LOADED BODIES		5. TYPE OF REPORT & PERIOD COVERED
7. AUTHOR(s) C. Brémond and A. J. Durelli		6. PERFORMING ORG. REPORT NUMBER
9. PERFORMING ORGANIZATION NAME AND ADDRESS Oakland University Rochester, MI 48063		8. CONTRACT OR GRANT NUMBER(s)
11. CONTROLLING OFFICE NAME AND ADDRESS Office of Naval Research Department of the Navy Washington, D.C. 20025		10. PROGRAM ELEMENT, PROJECT, TASK AREA & WORK UNIT NUMBERS
14. MONITORING AGENCY NAME & ADDRESS (if different from Controlling Office)		12. REPORT DATE June 1980
		13. NUMBER OF PAGES
		15. SECURITY CLASS. (of this report) Unclassified
		15a. DECLASSIFICATION/DOWNGRADING SCHEDULE
16. DISTRIBUTION STATEMENT (of this Report) Distribution of this report is unlimited		
17. DISTRIBUTION STATEMENT (of the abstract entered in Block 20, if different from Report)		
18. SUPPLEMENTARY NOTES		
19. KEY WORDS (Continue on reverse side if necessary and identify by block number) Contact stresses Grids Moiré Surfaces of Contact		
20. ABSTRACT (Continue on reverse side if necessary and identify by block number) The displacements which exist at the contact between two loaded bodies depend on the geometry of the surface of contact, the type of the loading and the property of the materials. A method has been developed to determine these displacements experimentally. A grid has been photographically printed on an interior plane of a transparent model of low modulus of elasticity. The displacements were recorded photographically and the analysis was conducted on the photographs of the deformed grids. Shears were determined from the change in angles. The precision of the measurements at the interface is		

DD FORM 1473

1 JAN 73

EDITION OF 1 NOV 65 IS OBSOLETE
S/N 0102-014-6001

SECURITY CLASSIFICATION OF THIS PAGE (When Data Entered)

estimated to be plus or minus 0.05 mm. Examples of application are given for the cases of loads applied normally and tangentially to a rigid cylindrical punch resting on a semi-infinite soft plate. Important observations can be made on the zones of friction and of slip. The proposed method is three-dimensional and the distributions can be obtained at several interior planes by changing the position of the plane of the grid. The limitations of the method are pointed out. The possibility of using gratings (12 to 40 lpmm) is considered, as well as the advantages of using moiré to analyze the displacements.

